DOI: 10.1002/ejic.200701231

Bis- and Tris(tetraazamacrocyclic) Copper Complexes with Disulfide Linkers

Monika Galińska,[a] Bohdan Korybut-Daszkiewicz,*[a,b] Urszula E. Wawrzyniak,[c] Renata Bilewicz,*[c] Pawel Śledź,[c] Radosław Kamiński,[d] Paulina Dominiak,[c] and Krzysztof Woźniak*[c]

Keywords: Polynuclear complexes / Multicenter complexes / Copper / Macrocyclic ligands

Di- and trinuclear title complexes, **2**Cu and **3**Cu, containing, respectively, two and three macrocyclic fragments bound by aliphatic linkers with the -S–S- moieties have been synthesized by using cystamine dihydrochloride in the presence of triethylamine. The structure of the **2**Cu complex in the solid state was confirmed by X-ray analysis. Two macrocyclic rings of **2**Cu form a rectangular cavity of size 17.18 Å [S19···S19 (1 – x, –y, –z)] × 3.62 Å. The shorter dimension of the cavity is the shortest observed in bis(macrocycle)s studied by us. The bis(macrocyclic) molecules in the crystal lattice are surrounded by PF_6^- ions and water molecules. Redox properties of the new compounds were determined by applying various voltammetric techniques. The macrocyclic architectures remained stable in nonaqueous solutions. For the bis- and tris(macrocyclic) compounds, the exchange of one electron takes place almost independently at each of the copper centers. The complexes were self- assembled at the gold surface to produce stable monolayer-modified electrodes. The immobilization of these highly charged cations on the electrode required the application of appropriate negative potentials during the self-assembly process.

Introduction

Self-assembly processes yielding polynuclear architectures from simple and stable complexes of transition-metal ions are important routes to new materials of unique magnetic and receptor properties.[1–6] They are also extensively studied as candidates for multilevel electronic devices scaled to the molecular level.[7–9] Synthesis of cyclidene dioxygen carriers and face-to-face bis(macrocyclic) ligands were described first by Busch and coworkers.[10–12] However, our choice are – contrary to the nonplanar [16]cyclidenes of Busch – the 14-membered macrocycles because of their planar structure. Additionally, we have recently shown that face-to-face bis(cyclidene)s linked by polymethylene chains form host–guest complexes with π-donor aromatic molecules.[6,13–15] This recognition phenomenon has been applied to synthesize novel mechanically interlocked supramolecules exhibiting intramolecular motion triggered by an appropriate potential.[13,14] Subtle changes in the molecular structure, for example, by varying the metal-to-metal distance or by changing the metal kind, allow the electron donor–acceptor properties of the system to be to modified.[16] Varying the linker length may introduce, or preclude, metal–metal interactions mediated through the bridging chains.[17] In several interactions, it is not the metal centers but the ligand electrons that are involved in the electronic interactions.[18,19]

In the present work, we modified the methylene linkers in the bis(cyclidene) molecular system by introducing -S–S- fragments (Figure 1). The aim of this modification was to obtain versatile compounds that can be used in solution or immobilized on gold surfaces.[20–23] Such structures should bind to gold supports by opening one of the linkers. In consequence, a face-to-face bis(macrocyclic) molecule should exhibit the ability of binding to the gold support by the opening of one of the linkers. It should also retain its receptor properties towards π-donating guests of appropriate size and shape. Self-assembled monolayers of such receptors would be important as building blocks for the construction of functional molecular devices in which the array of molecules of polymacrocyclic metal complexes can be switched on/off by the application of appropriate potentials and by changing the oxidation states of the metal centers.

---

[a] Cardinal Stefan Wyszyński University, College of Science, Department of Mathematics & Natural Science,
Dewajtis 5, 01-815 Warszawa, Poland
[b] Institute of Organic Chemistry Polish Academy of Sciences,
Kasprzaka 44/52, 01-224 Warszawa, Poland
[c] Department of Chemistry, Warsaw University,
Pasteura 1, 02-093 Warszawa, Poland
Fax: +48-22-8220211 ext. 345
E-mail: bilewicz@chem.uw.edu.pl
[d] Department of Chemistry, Warsaw University of Technology,
Noakowskiego 3, 00-664 Warszawa, Poland

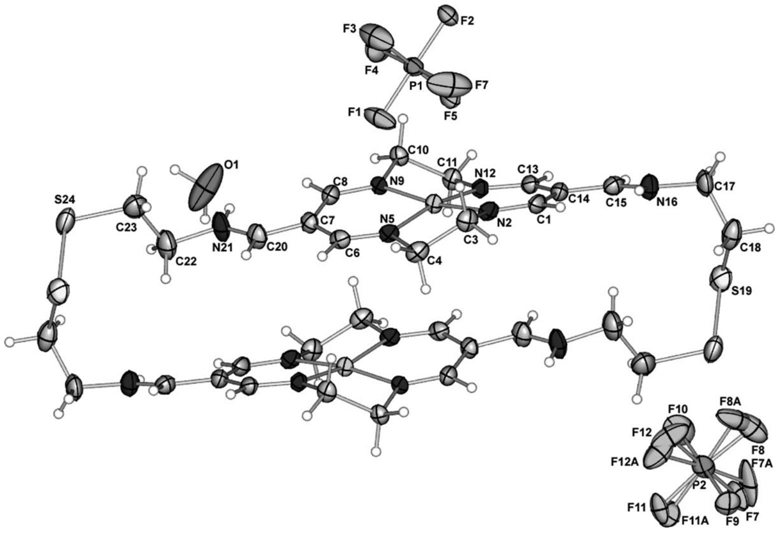

Figure 1. Atom labeling and atomic displacement parameters for **2**Cu.

Results and Discussion

Synthesis

The syntheses of complexes **2**Cu and **3**Cu are outlined in Scheme 1. Condensation of enol ether complex **1**Cu with cystamine dihydrochloride in the presence of triethylamine resulted in the formation of a mixture of di- and trinuclear complexes **2**Cu and **3**Cu, which were then separated by crystallization. Structures of isolated complexes were confirmed by elemental analysis and ESI mass spectrometry (Table 1 and Figure 1). The *m*/*z* values, as well as the ob-

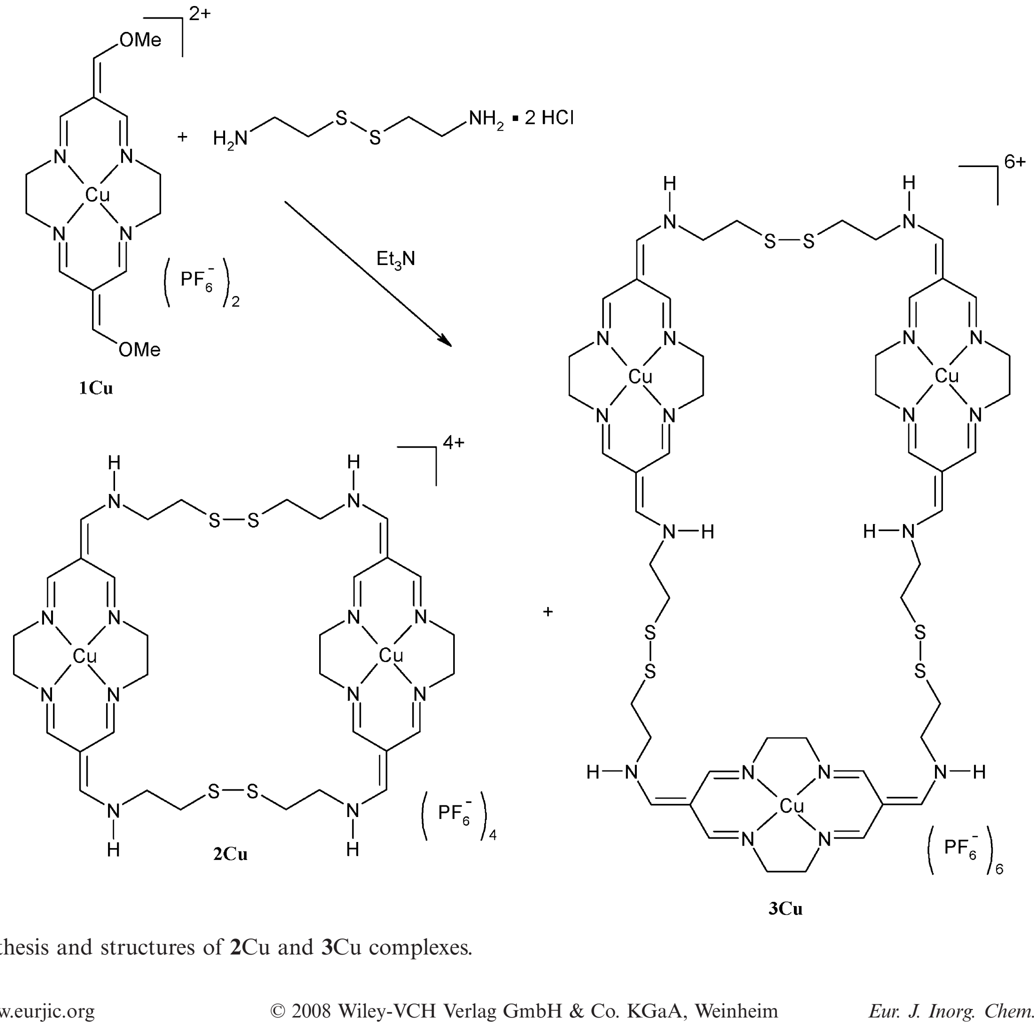

Scheme 1. Synthesis and structures of **2**Cu and **3**Cu complexes.

served isotopic profiles of the MS peaks, are consistent with the dimeric and trimeric structures of the **2**Cu and **3**Cu cations, respectively (Figure 2).

Table 1. MS (ESI) peaks of complexes **2**Cu and **3**Cu.

	2Cu (*n*) M = $[C_{32}H_{48}N_{12}S_4Cu_2]$	**3**Cu (*n*) M = $[C_{48}H_{72}N_{18}S_6Cu_3]$
$[M]^{n+}$	(4) 214.0 (53%)	(6) 214.0 (11%)
$[M + PF_6]^{n+}$	(3) 333.7 (100%)	(5) 285.6 (100%)
$[M - H]^{n+}$	(3) 285.0 (25%)	(5) 256.5 (60%)
$[M + 2\ PF_6]^{n+}$	(2) 573.0 (45%)	(4) 393.3 (95%)
$[M - 2\ H]^{n+}$	(2) 427.1 (16%)	(4) 320.3 (16%)
$[M + 3\ PF_6]^{n+}$	(1) 1291.0 (4%)	(3) 572.7 (25%)
$[M + 4\ PF_6]^{n+}$	–	(2) 931.6 (3%)

X-ray Structure of 2Cu

Complex **2**Cu crystallizes in the monoclinic $P2_1/c$ space group with half of the molecule as an independent part of the unit cell. Two macrocyclic fragments of the whole molecule are related to each other by the crystallographic center of symmetry. For an ORTEP view see Figure 1.

The Cu–N bond lengths are typical for the square-planar complexes with Cu^{II} cations and are 1.921(2) Å on average. The macrocyclic ring is close to planar, and the root mean square (RMS) deviation from the least-square plane of Cu(1), N(2), N(5), N(9), N(12), C(1), C(6), C(7), C(8), C(13), and C(14) is equal to 0.149 Å. The deviation from perfect planarity of the macrocyclic ring is caused by a 15° twist between the six-membered rings of the macrocycle. In each six-membered ring – along with the adjoining CH–NH–CH_2 fragment – a significant delocalization is observed, as seen from the average C–C bond lengths, 1.434(6) and 1.407(13) Å on average for the C(1)-C(14), C(6)C(7), C(7)C(8), C(13)C(14) and C(14)C(15), C(7)C(20) bonds, respectively. These bond lengths are in-between values for formally double and single C–C bonds (1.322 and 1.530 Å, respectively[24]). Such delocalization is typical for this type of compound.

In general, there can be *cis* or *trans* isomerism both on the macrocyclic units as well as on the ends of the aliphatic linkers. Here, two ethylene bridges from the same macrocyclic ring, as well as ethylene bridges from two different rings of the same bis(macrocyclic) molecule are in the *trans* orientation. The CH–NH–CH_2 fragments adopt the *trans* orientation relative to each other – when associated with the same macrocyclic ring – and the *cis* orientation relative to similar groups in the other macrocyclic ring of the same bis(macrocyclic) molecule.

Two macrocyclic rings of the molecule form a rectangular cavity of size 17.18 Å [S19···S19 ([1 – *x*, –*y*, –*z*] × 3.62 Å (distance between the two macrocyclic planes). The size of the cavity indicates a shortening of the distance between the two macrocyclic planes – unexpected for such a long linkers – and, as a result, unusual elongation in the perpendicular direction. Although, the shorter dimension of the cavity is the shortest observed in bis(macrocycle)s studied by us so far, the Cu···Cu separation (4.78 Å) is by ca. 0.3 Å larger than that for other bis(macrocycle)s with the shortest metal···metal contacts. A considerably large shift in the two macrocycles with respect to each other – 3.1 Å in the direction approximately along the Cu1C7 vector – is observed.

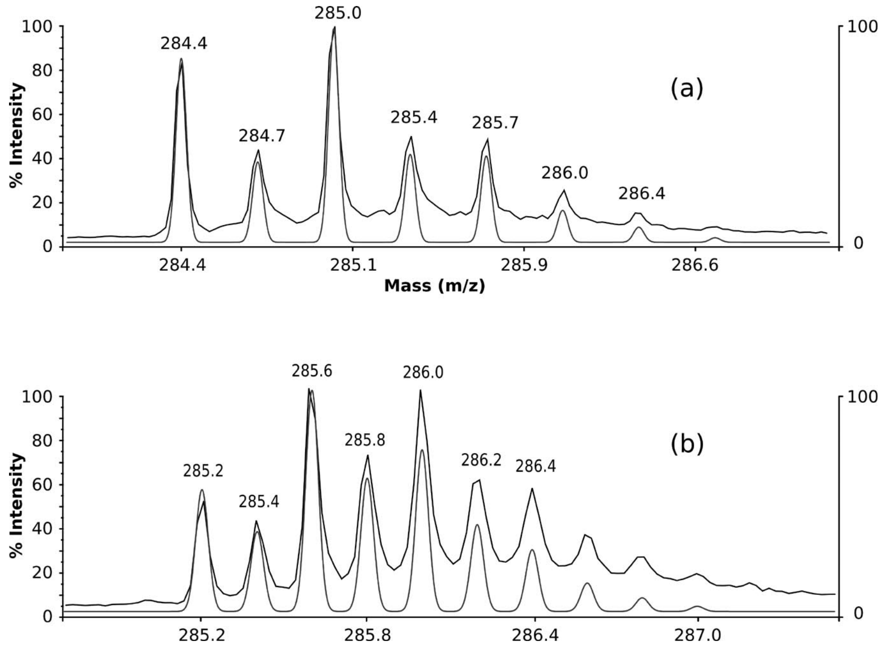

Figure 2. Experimental (black) and calculated (grey) profiles of the MS (ESI) peaks of complexes (a) **2**Cu – $[C_{32}H_{48}N_{12}S_4Cu_2 - H^+]^{3+}$; (b) **3**Cu – $[C_{48}H_{72}N_{18}S_6Cu_3 + (PF_6)^-]^{5+}$.

The bis(macrocyclic) molecules in the crystal lattice are surrounded by PF_6^- ions and water molecules. Water molecules form hydrogen bonding with N21 atoms with O1···N21 distance equal to 2.80 Å.

Molecules form 3D arrangement in such a way that four neighboring columns of molecules create channels along the *x* axis filled with anions that have some free space – this is why there is a positional disorder of the anions – whereas the projection along the *y* axis shows the layered nature of the structure (Figure 3). We would also like to stress that the bis(macrocyclic) moiety is very well shielded by the hexafluorophosphate anions and form a layer around the bis(macrocycle).

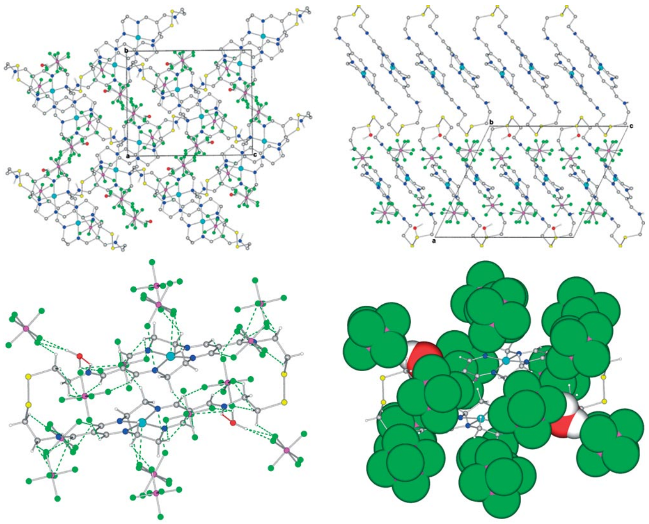

Figure 3. Projection of the crystal lattice of **2**Cu along (a) the *x* axis; (b) the *y* axis; (c) and (d) intermolecular interactions of the bis(macrocycle) and the closest shell of counterions.

Electrochemistry

Comparison of the redox properties of the bis- and tris(macrocyclic) complexes in acetonitrile (AN) solution was performed. Bis- and tris(macrocyclic complexes) **2**Cu and **3**Cu (Scheme 1) are soluble in acetonitrile (AN) and *N*,*N*-dimethylformamide (DMF), but not in chloroform or ethanol.

Cyclic voltammograms of **2**Cu and **3**Cu (Figure 4) indicate close to reversible redox processes involving exchange of two and three electrons, respectively. The peak current ratios are close to one, whereas the peak-to-peak separation only slightly exceeds the value expected for the ideally reversible 1e process. The characteristics of the redox processes studied by cyclic voltammetry are presented in Table 2. The $E_{1/2}$ potential approximated as $(E_{pc} + E_{pa})/2$ for **3**Cu is less positive than that for **2**Cu and the peak current is larger, as expected for the increasing number of electroactive subunits. Although we have not obtained the 3D structure of **3**Cu, we suspect that the weaker donor abilities of **3**Cu result from less effective packing of macrocycle units within the tris(macrocycle) moiety.

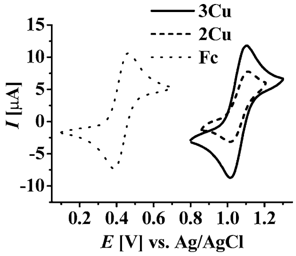

Figure 4. Cyclic voltammograms for 5×10^{-4} M **2**Cu and **3**Cu in 0.1 M TBAHFP/AN solution, v = 50 mV s^{-1}.

Table 3 shows the results obtained by differential pulse (DP) voltammetry. From the plots of the peak current versus square root of scan rate, the diffusion coefficients of the compounds were calculated on the basis of the Randles–Sevčik Equation [Equation (1)].[25]

$$I_p = 2.27\times10^5 n^{3/2} D^{1/2} A v^{1/2} C^0_{ox} \qquad (1)$$

where I_p [A] is the peak current, n is the number of electrons, A [cm^2] is the electrode area, v [V s^{-1}] is the scan rate, and C^0_{ox} [mM] is the concentration of the complex.

The diffusion coefficients are equal to 1.86×10^{-6} and 1.11×10^{-6} cm^2 s^{-1} for **2**Cu and **3**Cu, respectively.

The voltammograms for **2**Cu were fitted to an E1–E2 mechanism described by Equation (2).

$$\mathrm{Cu^{II}Cu^{II}} - \mathrm{e} \xrightarrow{E_1} \mathrm{Cu^{II}Cu^{III}} - \mathrm{e} \xrightarrow{E_2} \mathrm{Cu^{III}Cu^{III}} \qquad (2)$$

An additional equilibrium is the comproportionation [Equation (3)].

Table 2. Characteristics of the cyclic voltammograms for 5×10^{-4} M **2**Cu and **3**Cu in 0.1 M TBAHFP/AN solution.

	2Cu					3Cu				
V [mV s^{-1}]	E_{pa}[a] [V]	I_{pa}[a] [μA]	E_{pc}[a] [V]	$E_{1/2}$[b] [V]	$E_{pa} - E_{pc}$ [V]	E_{pa}[a] [V]	I_{pa}[a] [μA]	E_{pc}[a] [V]	$E_{1/2}$[b] [V]	$E_{pa} - E_{pc}$ [V]
10	1.111 ±0.002	3.91 ±0.13	1.030 ±0.002	1.071 ±0.002	0.081 ±0.004	1.098 ±0.001	5.74 ±0.22	1.014 ±0.001	1.056 ±0.001	0.084 ±0.002
50	1.110 ±0.001	7.92 ±0.45	1.031 ±0.001	1.071 ±0.001	0.079 ±0.002	1.102 ±0.002	11.98 ±0.62	1.014 ±0.001	1.058 ±0.002	0.088 ±0.003
100	1.112 ±0.002	12.09 ±1.44	1.029 ±0.002	1.071 ±0.002	0.083 ±0.004	1.104 ±0.001	17.3 ±0.95	1.010 ±0.001	1.057 ±0.001	0.094 ±0.002

[a] The mean value for three measurements. [b] Approximated as $(E_{pc} + E_{pa})/2$.

$$\mathrm{Cu^{II}Cu^{II} + Cu^{III}Cu^{III} \leftrightarrow 2Cu^{II}Cu^{III}} \quad (3)$$

The comproportionation constant was evaluated on the basis of Equation (4).[26]

$$K_{\mathrm{com}} = \exp\left[\frac{(\Delta E)\times F}{RT}\right] \quad (4)$$

where ΔE is the difference in the formal potentials for the 1e processes at two copper centers, F is the Faraday constant 96500 C, R is the gas constant 8.31 J mol^{-1} K^{-1}, and T is temperature (298 K).

The value of ΔE was 35 mV, which leads to K_{com} ca. 3.9. This result points to noninteractive copper centers in this complex. The expected value of formal potential separation for two independent identical electroactive sites is ca. 35.6 mV, whereas for the three centers it is equal to 57 mV.[26]

The differential pulse and square-wave (SW) voltammograms for both compounds are shown in Figure 5 and their characteristics are depicted in Tables 3 and 4.

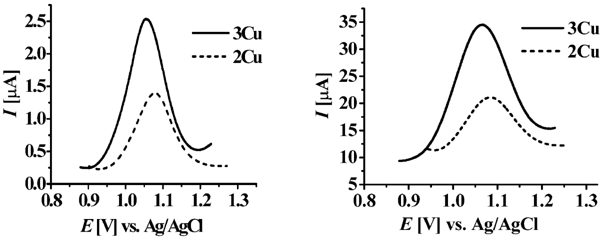

Figure 5. DP (a) and SW (a) voltammograms for 5×10^{-4} M **2**Cu and **3**Cu in 0.1 M TBAHFP/AN solution; (a) ΔE = 10 mV, (b) f = 50 Hz.

The $b_{1/2}$ width of the peak at half height is slightly larger than the 90.6 mV expected for a 1e reversible process. However, the peak current indicates that 2 and 3 electrons are exchanged. This confirms that the electron is exchanged almost independently at each of the copper centers.

Redox Behavior of Bis- and Tris(macrocyclic) Complexes Self-Assembled on Gold Electrode

The gold electrode was immersed in a deoxygenated 1-mM solution of **2**Cu in 0.1 M $\mathrm{LiClO_4}$/AN for 2 h. The macrocyclic complex was self-assembled at the gold surface when a –0.5 V potential was applied to the electrode. Without potential application, the compound remained in the solution owing to the high charge of the molecule precluding the self assembly process. This charge had to be compensated by the opposite charge of the electrode. After 2 h of self-assembly, the electrode was rinsed with AN and placed in the electrochemical cell containing only deoxygenated supporting electrolyte solution − 0.1 M TBAHFP/AN. The cyclic voltammograms reveal the presence of surface-bound bis(macrocylic) complex (Figure 6). Probably, one of the -S–S- bonds is broken in the self-assembly process, which allows the molecule to anchor to the surface. Adsorption is known to be the first step in the process of immobilization of the -S–S- bridged compounds. It is then followed by cleavage of the appropriate bonds and formation of a new bond to the gold surface. Therefore, simultaneous cleavage of all -S–S- bonds for such rigid molecule as ours is rather unfavorable. We do not have, however, direct

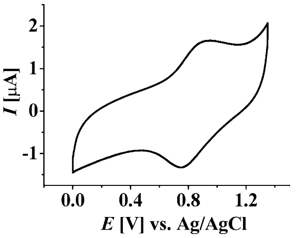

Figure 6. Monolayers of **2**Cu on gold electrode self-assembled for 2 h under –0.5 V from 1 mM **2**Cu solution 0.1 M TBAHFP/AN. Cyclic voltammogram recorded in 0.1 M TBAHFP/AN solution, scan rate: 0.5 V s^{-1}.

Table 3. Characteristics of DP voltammograms for **2**Cu and **3**Cu.

	2Cu			3Cu		
ΔE [mV]	E_p [V]	I_p [μA]	$b_{1/2}$	E_p [V]	I_p [μA]	$b_{1/2}$
5	1.079 ± 0.001	0.83 ± 0.16	0.094 ± 0.004	1.058 ± 0.002	1.37 ± 0.35	0.104 ± 0.002
10	1.079 ± 0.002	1.22 ± 0.18	0.105 ± 0.002	1.055 ± 0.001	2.13 ± 0.13	0.107 ± 0.001
15	1.077 ± 0.000	1.57 ± 0.12	0.103 ± 0.001	1.056 ± 0.001	2.71 ± 0.10	0.110 ± 0.001
20	1.078 ± 0.001	1.23 ± 0.34	0.107 ± 0.001	1.054 ± 0.001	3.29 ± 0.11	0.112 ± 0.001
25	1.073 ± 0.001	3.66 ± 0.62	0.098 ± 0.002	1.054 ± 0.001	3.74 ± 0.06	0.114 ± 0.001
50	1.070 ± 0.001	6.92 ± 0.81	0.102 ± 0.001	0.045 ± 0.002	7.46 ± 0.1	0.118 ± 0.001

Table 4. Characteristics of SW voltammograms for **2**Cu and **3**Cu.

		2Cu			3Cu	
f [Hz]	E_p [V]	I_p [μA]	$b_{1/2}$	E_p [V]	I_p [μA]	$b_{1/2}$
8	1.069 ± 0.006	8.18 ± 0.69	0.106 ± 0.004	1.059 ± 0.001	20.93 ± 1.47	0.126 ± 0.001
10	1.075 ± 0.002	10.16 ± 1.3	0.109 ± 0.003	1.058 ± 0.001	19.37 ± 0.57	0.128 ± 0.001
50	1.075 ± 0.001	18.23 ± 0.43	0.109 ± 0.001	1.065 ± 0.0005	22.3 ± 0.70	0.133 ± 0.002
60	1.074 ± 0.002	19.03 ± 0.97	0.108 ± 0.001	1.060 ± 0.001	24.03 ± 0.54	0.136 ± 0.003
100	1.075 ± 0.001	14.53 ± 0.37	0.103 ± 0.001	1.063 ± 0.002	23.07 ± 0.77	0.137 ± 0.003
120	1.076 ± 0.001	12.30 ± 0.7	0.101 ± 0.001	1.063 ± 0.002	23.37 ± 0.47	0.142 ± 0.001

proof of this, as the coverage of the electrode is far less than a full monolayer. Better-developed cyclic voltammograms are obtained when the Rubinstein et al.[27] approach is used in the self-assembly procedure. It involves an initial self-assembly of an alkanethiol monolayer exchanged in the following self-assembly step by the compound of interest (in our case). The resulting surface waves for **3**Cu are shown in Figure 7. The bis- and tris(macrocycle) modified gold surfaces are stable. The formal potential obtained for immobilized **2**Cu or **3**Cu differ by ca. 20 mV, and the latter appears at less-positive potentials. The difference for the soluble complexes was similar. Better adsorption and, hence, much better developed voltammograms are obtained for neutral macrocyclic complexes instead of the highly charged macrocycles described in this paper. Work in this direction is in progress. Our approach opens a new route for the construction of more complex nanostructures such as rotaxanes or catenanes on the surfaces of electrodes.

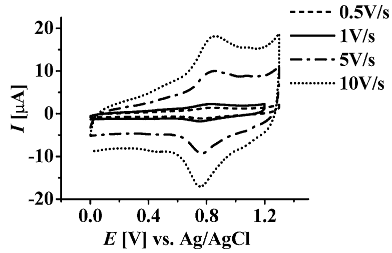

Figure 7. Cyclic voltammograms recorded at increasing scan rates for **3**Cu self-assembled under –0.5 V on the gold electrode surface pretreated according to the Rubinstein et al. procedure[26] (details in the text). Solution: 0.1 м TBAHFP/AN.

Conclusions

Application of cystamine dihydrochloride in the presence of triethylamine resulted in the formation of mixture of di- and trinuclear complexes, **2**Cu and **3**Cu, containing two and three macrocyclic fragments bound by linkers with the -S–S- built-in units. The structure of the **2**Cu complex in the solid state was confirmed by X-ray analysis. Two macrocyclic rings of **2**Cu form a rectangular cavity of size 17.18 Å [S19···S19 (1 – *x*, –*y*, –*z*)] × 3.62 Å. The shorter dimension of the cavity is the shortest observed in bis(macrocycle)s studied by us so far. The bis(macrocyclic) molecules in the crystal lattice are surrounded by PF_6^- ions and water molecules.

Voltammetric studies of the new complexes dissolved in AN solutions proved that the macrocyclic architectures remain stable in the nonaqueous solutions. For the bis- and tris(macrocyclic) compounds, the exchange of one electron takes place almost independently at each of the copper centers. These highly charged complexes may be self-assembled at the gold surface by breaking one of the -S–S- bonds when an appropriate negative potential is applied to the electrode. Such gold surfaces decorated with polymacrocyclic complexes are stable and reproducible; thus, this procedure opens a new route for constructing molecular devices based on triggered polymacrocyclic units, for example, rotaxanes and catenanes bound to a conducting support.

Experimental Section

Materials and Instrumentation: The solvents and reagents used in these studies were reagent grade or better. Acetonitrile was dried with P_2O_5 and distilled under an atmosphere of argon. 6,13-Bis(methoxymethylidene)-1,4,8,11-tetrazacyclotetradeca-4,7,11,14-tetraenecopper(II) hexafluorophosphate (**1**Cu) was synthesized according to the previously published procedures.[6] Electrospray ionization (ES) mass spectra were recorded with a Mariener Perseptive Biosystem spectrometer. IR spectra (paraffin oil mulls) were measured with a Perkin–Elmer Spectrum 2000 spectrometer.

Preparation of 2Cu and 3Cu: Cystamine dihydrochloride (0.225 g, 1 mmol) and triethylamine (0.278 mL, 2 mmol) were dissolved in a mixture of dry acetonitrile (35 mL) and methanol (10 mL). Copper macrocyclic complex **1**Cu (0.630 g, 1 mmol) was added to the solution, and the mixture was stirred at room temperature. After 0.5 h, a solution of NH_4PF_6 (1.5 g) in methanol (20 mL) was added, followed by the addition of water (100 mL) acidified with concentrated hydrochloric acid (1 mL). The organic solvent was removed by rotary evaporation, and the remaining mixture was placed in a refrigerator to complete crystallization. A pink precipitate was filtered off, dissolved in acetonitrile containing a small amount of NH_4PF_6, and diluted with ethanol and water. After 3 d, product **2**Cu (0.388 g, 54%) precipitated upon slow evaporation of the solvents, and it was filtered off and washed with ethanol. The remaining filtrate was left in open flask for the next week and after evaporation of ca. 90% of solvents another crop of pink crystals was filtered off. The second fraction was later proved by MS (ESI) to contain trimer **3**Cu (0.031 g, 4%). Data for **2**Cu: $C_{32}H_{48}Cu_2N_{12}S_4{\cdot}(PF_6)_4{\cdot}2H_2O$ (1472.0): calcd. C 26.1, H 3.6, N 11.4; found C 26.5, H 3.5, N 11.6. IR (nujol): $\tilde{\nu}$ = 3372 (s), 1665 (s), 1615 (vs), 1585 (s), 842 (vs), 556 (s) cm^{-1}. Data for **3**Cu: $C_{48}H_{72}N_{18}S_6Cu_3{\cdot}(PF_6)_6$ (2154.0): calcd. C 26.8, H 3.4, N 11.7; found C 26.8, H 3.9, N 11.5. IR (nujol): $\tilde{\nu}$ = 3379 (s), 1669 (s), 1615 (vs), 1570 (s), 839 (vs), 556 (s) cm^{-1}.

Voltammetry: Linear scan, differential pulse, and square-wave voltammetry experiments were done by using an Autolab potentiostat (ECO Chemie, Netherlands) in three-electrode arrangement with a silver/silver chloride (Ag/AgCl) as the reference, platinum foil as the counter electrode, and glassy carbon electrode (GCE, BAS, A = 0.0706 cm^2) as the working electrode. In the self-assembly experiments, Au, BAS electrodes, A = 0.02 cm^2 was used. The reference electrode was separated from the working solution by electrolytic bridge filled with 0.1 м TBAHFP/AN solution. The reference electrode potential was calibrated by using ferrocene electrode process in the same TBAHFP/AN solution. An acetonitrile (AN) solution containing 0.1 м tetrabutylammonium hexafluorphosphate (TBAHFP) was used as the supporting electrolyte solution. Argon was used to deaerate the solution and argon blanket was maintained over the solution during the experiments.

X-ray Diffraction: Measurements were performed with a Kuma KM4CCD κ-axis diffractometer with graphite-monochromated Mo-K_α radiation and equipped with an Oxford Cryosystems nitrogen gas-flow apparatus. The crystal was positioned at 62 mm from the KM4CCD camera. 600 frames were measured at 1° intervals with a counting time of 25 sec. The data were corrected for Lorentz and polarization effects. No absorption correction was applied. Data reduction and analysis were carried out with the Oxford Diffraction Ltd. suit of programs.

The structure was solved by direct methods[28] and refined by using SHELXL.[29] The refinement was based on F^2 for all reflections except those with very negative F^2. Weighted R factors wR and all goodness-of-fit S values are based on F^2. Conventional R factors are based on F with F set to zero for negative F^2. The $F_o^2>2\sigma(F_o^2)$ criterion was used only for calculating R factors and is not relevant to the choice of reflections for the refinement. The R factors based on F^2 are about twice as large as those based on F. Scattering factors were taken from Tables 6.1.1.4 and 4.2.4.2 in ref.[21].

Non-hydrogen atoms were refined anisotropically. Both PF_6^- ions show signs of rotational disorder. For the P2 ion two different positions of F7, F8, F11 and F12 atoms where refined with occupancy factors of 0.57 and 0.43. There is one strong residual peak of $2.00\,\mathrm{e\,\AA^{-3}}$, 1.24 Å from S24 atom, for which no reasonable model of disorder could be found. Hydrogen atoms of macrocyclic molecule were placed in idealized positions and refined using a riding model with $U_{iso} = 1.2U_{eq}$. Positions of hydrogen atoms from water molecule were found by difference electron density Fourier synthesis and constrained during refinement to the O–H distance of 0.964 Å with $U_{iso} = 1.2U_{eq}$. Crystal data for **2**Cu: $C_{32}H_{52}Cu_2N_{12}O_2F_{24}P_4S_4$, $fw = 1472.06$; $T = 100(2)$ K; $\lambda = 0.71073$ Å; monoclinic; space group, $P2_1/c$; unit cell dimensions: $a = 14.7401(6)$ Å, $b = 12.4809(4)$ Å, $c = 16.5508(5)$ Å, $\alpha = 90°$, $\beta = 116.148(3)°$, $\gamma = 90°$; $V = 2733.23(16)$ Å^3; $Z = 2$; $D_{calcd.} = 1.789\,\mathrm{Mg\,m^{-3}}$; absorption coefficient: $1.176\,\mathrm{mm^{-1}}$; $F(000) = 1484$; crystal size: $0.25\times0.25\times0.06\,\mathrm{mm^3}$; θ range for data collection: 2.74–27.5°; index ranges: $-19 < h < 19$, $-15 < k < 15$, $-21 < l < 21$; reflections collected: 48320/unique 5959 [R(int) = 0.0448]; absorption correction − semiempirical from equivalents; max. and min. transmission: 0.932 and 0.722; refinement method − full-matrix least-squares on F^2; goodness-of-fit on $F^2 = 1.072$; data/restraints/parameters 5959/157/404; final R indices [$I > 2\sigma(I)$]: $R1 = 0.0446$, $wR2 = 0.1229$; R indices (all data): $R1 = 0.0673$, $wR2 = 0.1301$; weight: $1/[\sigma^2(F_o^2) + (0.0775P)^2 + 0.28P]$, where $P = [\max(F_o^2, 0) + 2F_c^2]/3$; largest diffraction peak and hole: 2.00 and $-1.10\,\mathrm{e\,\AA^{-3}}$.

CCDC-667536 (for **2**Cu) contains the supplementary crystallographic data for this paper. These data can be obtained free of charge from The Cambridge Crystallographic Data Centre via www.ccdc.cam.ac.uk/data_request/cif.

Acknowledgments

This work was supported through grant by the Ministry of Science and Higher Education (Project N20407432/2022). The X-ray measurements were undertaken in the Crystallographic Unit of the Physical Chemistry Laboratory at the Chemistry Department of the University of Warsaw.

---

[1] J.-P. Sauvage (Ed.). *Molecular Machines and Motors, Structure Bonding*, Springer, Berlin, **2001**, vol. 99.
[2] V. Balzani, M. Venturi, A. Credi. *Molecular Devices and Machines*, Wiley-VCH, Weinheim, **2003**.
[3] S. Bonnet, J.-P. Collin, M. Koizumi, P. Mobian, J.-P. Sauvage, *Adv. Mater.* **2006**, *18*, 1239–1250.
[4] E. R. Kay, D. A. Leigh, F. Zerbetto, *Angew. Chem. Int. Ed.* **2007**, *46*, 72–191.
[5] B. Champin, P. Mobian, J.-P. Sauvage, *Chem. Soc. Rev.* **2007**, *36*, 358–366.
[6] B. Korybut-Daszkiewicz, A. Wieckowska, R. Bilewicz, S. Domagala, K. Wozniak, *J. Am. Chem. Soc.* **2001**, *123*, 9356–9366.
[7] M. Ruben, E. Breuning, J.-P. Gisselbrecht, J.-M. Lehn, *Angew. Chem. Int. Ed.* **2000**, *39*, 4139–4142.
[8] M. Ruben, E. Breuning, M. Barboiu, J.-P. Gisselbrecht, J.-M. Lehn, *Chem. Eur. J.* **2003**, *9*, 291–299.
[9] E. Baranoff, F. Barigelletti, S. Bonnet, J. P. Collin, L. Flamigni, P. Mobian, J.-P. Sauvage, *Struct. Bonding (Berlin)* **2007**, *123*, 41–78.
[10] D. H. Busch, *Inorg. Chem.* **1986**, *25*, 3000–3006.
[11] D. H. Busch in *Comprehensive Supramolecular Chemistry* (Ed.: J.-M. Lehn), Pergamon Press, Oxford, **1996**, vol. 9, ch. 1.
[12] D. H. Busch, N. W. Alcock, *Chem. Rev.* **1994**, *94*, 585–623.
[13] a) B. Korybut-Daszkiewicz, A. Wieckowska, R. Bilewicz, S. Domagala, K. Wozniak, *Angew. Chem. Int. Ed.* **2004**, *43*, 1668–1672; b) B. Korybut-Daszkiewicz, A. Wieckowska, R. Bilewicz, S. Domagala, K. Wozniak, *Angew. Chem.* **2004**, *116*, 1700–1704.
[14] R. Bilewicz, B. Korybut-Daszkiewicz, A. Rogowska, J. Szydłowska, A. Więckowska, S. Domagała, K. Woźniak, *Electroanalysis* **2005**, *17*, 1463–1470.
[15] S. Domagala, A. Wieckowska, J. Kowalski, A. Rogowska, J. Szydlowska, B. Korybut-Daszkiewicz, R. Bilewicz, K. Wozniak, *Chem. Eur. J.* **2006**, *12*, 2967–2981.
[16] A. Wieckowska, R. Bilewicz, S. Domagala, K. Wozniak, B. Korybut-Daszkiewicz, A. Tomkiewicz, J. Mrozinski, *Inorg. Chem.* **2003**, *42*, 5513–5522.
[17] A. Vlcek Jr, in *Electron Transfer in Chemistry* (Ed.:V. Balzani), Wiley-VCH, Weinheim, **2001**, vol. 2, pp. 804–877.
[18] M. Marcaccio, F. Paolucci, C. Paradisi, S. Roffia, C. Fontanesi, L. J. Yellowlees, S. Serroni, S. Campagna, G. Denti, V. Balzani, *J. Am. Chem. Soc.* **1999**, *121*, 10081–10091.
[19] M. Ruben, E. Breuning, M. Barboiu, J.-P. Gisselbrecht, J.-M. Lehn, *Chem. Eur. J.* **2003**, *9*, 291–299.
[20] R. A. Bissel, E. Cordova, A. E. Kaifer, J. F. Stoddart, *Nature* **1994**, *369*, 133–137.
[21] A. E. Kaifer, M. Gomez-Kaifer, *Supramolecular Electrochemistry*, Wiley VCH, New York, **1999**, pp. 142–161.
[22] S. Sek, A. Misicka, K. Swiatek, E. Maicka, *J. Phys. Chem. B* **2006**, *110*, 19671–19677.
[23] A. Wieckowska, M. Wisniewska, S. Sek, M. Chrzanowski, J. Kowalski, B. Korybut-Daszkiewicz, R. Bilewicz, *J. Pure Appl. Chem.* **2007**, *79*, 1077–1085.
[24] A. J. C. Wilson (Ed.), *International Tables for Crystallography*, Kluwer, Dordrecht, **1992**, vol. C.
[25] Z. Galus. *Fundamentals of Electrochemical Analysis*, 2nd ed., Polish Scientific Publishers, Warsaw, **1994**.
[26] J.-B. Flanagan, S. Margel, A. J. Bard, F. C. Anson, *J. Am. Chem. Soc.* **1978**, *100*, 4248–4253.
[27] M. Wanunu, A. Vaskevich, J. Rubinstein, *Izrael Journal. Chem.* **2005**, *45*, 337–344.
[28] G. M. Sheldrick, *Acta Crystallogr. Sect. A* **1990**, *46*, 467–473.
[29] G. M. Sheldrick, *SHELXL93: Program for the Refinement of Crystal Structures*, University of Göttingen, Germany.

Received: November 16, 2007